



## Impedance Spectroscopic Studies of NiMgCuZn Ferrites

Varalaxmi N\*

Department of Physics, Kakatiya University, Warangal, Telangana, India

### Abstract

A series of Ni substituted MgCuZn polycrystalline ferrite were prepared by a high energy ball-milling followed by the standard double sintering ceramic technique to investigate the impedance spectroscopic studies, within the frequency and temperature range of 100 Hz to 1 MHz at various temperatures within the range of 30°C-490°C these studies were carried out. XRD and SEM patterns were taken to confirm the formation of single phase cubic structure and the grain size. The complex-plane impedance spectra indicates that the material can be represented by both bulk and the grain boundary phenomena at high and low frequencies respectively as two semi-circular arcs was observed. The results of the real impedance  $Z'$  and imaginary part  $Z''$  at low frequencies are discussed as being attributed to the interfacial polarization; The results of real impedance  $Z'$  and imaginary part  $Z''$  at various frequencies are discussed along with the dielectric properties of temperature and frequency.

**Keywords:** X-ray diffraction; SEM patterns; Ferrimagnetic materials; Impedance spectroscopy; Dielectric properties

### Introduction

Semiconductor natured polycrystalline ferromagnetic ceramics with spinel structure are most sought materials and drawn considerable attention due to their interesting electrical properties of low eddy currents and dielectric losses.

Recently, in particular polycrystalline ferrites, they have found innumerable high potential applications for their use in wide ranges of frequencies extending from a microwave applications to radio frequencies, which are also applicable to many electromagnetic devices, such as magnetic cores of read-write heads for high speed digital tape and disk recorders due to the low electrical conductivity as compared to that of magnetic materials.

Ferrites have high electrical resistivity and permeability which is frequency dependent. One of the most important properties of the ferrites is electrical conductivity; hence, the electrical conductivity behaviour gives valuable information about their conduction mechanism. The order of magnitude of conductivity influences greatly on the dielectric and magnetic behavior of the ferrites and also depends on method of preparation. In ceramic preparation method, it depends on the various chemical compositions, sintering temperature, sintering time, and the type of substitution [1,2]. In the investigation of researchers, it was reported that ferrites sintered in the air are characterized from highly conductive grains separated by highly resistive grain boundaries [3]. So far, ferrites have been widely used in many magnetic devices than those of soft magnetic alloys, because, the electrical properties of ferrites are mostly influenced by the grain boundaries, due to their high electrical resistivities and dielectric constant as well as low dielectric loss makes them very important materials and extensively used. Many more researchers investigated so far on various substitutions and studied the magnetic, dielectric and thermal properties of ferrites such as Ni-Co [4] and Ni-Cu mixed ferrites [5,6] to achieve the desired properties [7-15].

Studies on Impedance spectroscopy of ferrites materials is a new technique which characterizes many of the electrical properties and their interfaces with electronically conducting electrodes. The importance and usefulness of impedance spectroscopy studies lies in the ability to distinguish the dielectric and electrical properties of individual contributions of components under investigation, in

which the technique ensures separation among the bulk, grain, grain boundaries and electrode electrolyte interface properties. It also had a great ability to analyze the relaxation phenomenon occurring in the materials. It can also be used in order to investigate the mobile charges in bulk (or) interfacial regions of any kind of solids (or) Ionic, semi-conductive, mixed electronic-ionic and even insulators (dielectrics).

Few authors carried out studies on impedance spectra [16-19], but the author found that there is no investigation reported on NiMgCuZn ferrites. Hence, in the present investigation the author carried out the studies on Ni substituted MgCuZn ferrites and the results are reported.

### Experimental Details

#### Preparation of samples

The ferrite composition with generic formula  $\text{Ni}_x\text{Mg}_{0.6-x}\text{Cu}_{0.1}\text{Zn}_{0.3}\text{Fe}_2\text{O}_4$  with  $x=0.0, 0.1, 0.2$  and  $0.3$  were prepared by the conventional ceramic double sintering method. To synthesize these ferrites High-energy ball-milling has been used, this method possesses several advantages such as time gain, homogeneity and energy.

NiMgCuZn ferrites were prepared by choosing the stoichiometric proportions of analytical grade NiO, MgO, CuO, ZnO and  $\text{Fe}_2\text{O}_3$  were taken intimately mixed in agate mortar and presintered for 8 hrs and then ball milled in Restch PM 200 planetary ball mill in acetone medium using polyethylene jars with iron balls ( $\phi = 5\text{mm}$ ) for 24 h. The powder was then pressed into green pellets of 1.2 cm diameter and 0.2 cm thickness using PVA solution as a binder in a hydraulic press at a pressure of 150 MPa. These compacted bodies were finally sintered at 1250°C for 2 h in a programmable furnace and were cooled to room temperature at the rate of 80°/h. Sufficient care was taken to avoid the zinc loss during the sintering process by placing these compacted pellets in a closed alumina crucible with excess of Zn atmospheric powder.

**\*Corresponding author:** Dr. Narla Varalaxmi, Assistant Professor, Department of Physics, Kakatiya University, Warangal, Telangana, India, Tel: +91- 9848290078; E-mail: [dr.narlasharma@gmail.com](mailto:dr.narlasharma@gmail.com)

**Received** April 30, 2019; **Accepted** May 30, 2019; **Published** June 06, 2019

**Citation:** Varalaxmi N (2019) Impedance Spectroscopic Studies of NiMgCuZn Ferrites. J Material Sci Eng 8: 527.

**Copyright:** © 2019 Varalaxmi N. This is an open-access article distributed under the terms of the Creative Commons Attribution License, which permits unrestricted use, distribution, and reproduction in any medium, provided the original author and source are credited.

## Identification of phase

All the samples were structurally characterized using Philips high resolution X-ray diffraction system (Model PW-1710) with monochromatised Cu K (radiation at room temperature. The Scanning electron micrographs were recorded with the help of SEM (Philips XL30ESEM) instrument. Thermally etched samples were taken for making the SEM specimens. The samples were mounted on brass studs with double sided adhesive tape and coated with Au-Pd alloy of 120-150 Å thickness of argon ambient atmosphere of 8-10 Pascal.

## Characterization

Dense ferrite samples were polished to obtain a smooth surface and coated with a silver paste for good ohmic contacts on either side. The temperature variation in DC resistivity was measured by the two-probe method with in the range 30 to 490°C [8]. The frequency dependence on capacitance and dissipation factor ( $\tan\delta$ ) in the range 100 Hz to 1MHz was studied using a precision impedance analyzer LCR bridge of model Hioki 3532-50 Hi-tester. The AC conductivity was calculated using room-temperature dielectric data. The magnitude of complex impedance measurements  $Z'$  and  $Z''$  were recorded directly at 10°C temperature intervals in the temperature range 30 to 350°C at different frequencies in the range 100 Hz to 1MHz with the help of a low frequency impedance analyzer Hioki LCR Hitester model 3532-50 and a computer interfaced tubular furnace so as to calculate the AC conductivities of the samples.

## Result and Discussions

### Structural characterization

X-ray diffraction patterns of the ferrites studied in the present

investigation were shown in Figure 1. The existence of broadening peaks indicates the formation of single phase cubic spinel structures. The SEM patterns of the ferrite samples are shown in Figure 2. As observed from the SEM microphotographs, pure MgCuZn ferrite has larger grain diameters when compared to Ni substituted MgCuZn ferrites. It seems that by substitution of Ni concentration in MgCuZn ferrites, the densities are decreasing linearly.

With the addition of Ni content the lattice parameter varies from 8.374 to 8.234 Å. This variation can be ascribed to the difference in ionic sizes of the component ions. When compared to ionic sizes of  $\text{Mg}^{2+}$  (0.68Å),  $\text{Cu}^{2+}$  (0.70Å),  $\text{Zn}^{2+}$  (0.74Å) and  $\text{Fe}^{3+}$  (0.67Å) ions,  $\text{Ni}^{2+}$  ions has larger ionic radii (0.78 Å), hence there is a decrease in lattice parameter. 1.25 µm is the average particle size. The observed grain size increases slightly with the addition of nickel, hence the increased grain size results with an increase in mean free paths of the electrons which causes the change in resistivity.

### Impedance spectroscopy studies

The variation of AC and DC electrical conductivities for Ni substituted MgCuZn ferrites as a function of temperature and frequency for all the samples were discussed earlier [8] and dielectric properties of NiMgCuZn ferrites were also discussed earlier [20].

In general ferrimagnetic materials possess good electrical and magnetic properties. Hence, impedance spectroscopy is the tool for their investigation. The results of the present ferrites investigated were discussed at different temperatures and frequencies. At low frequencies both real impedance ( $Z'$ ) and imaginary part ( $Z''$ ) are attributed to the interfacial polarization and Debye relaxation is dominant at high frequencies.

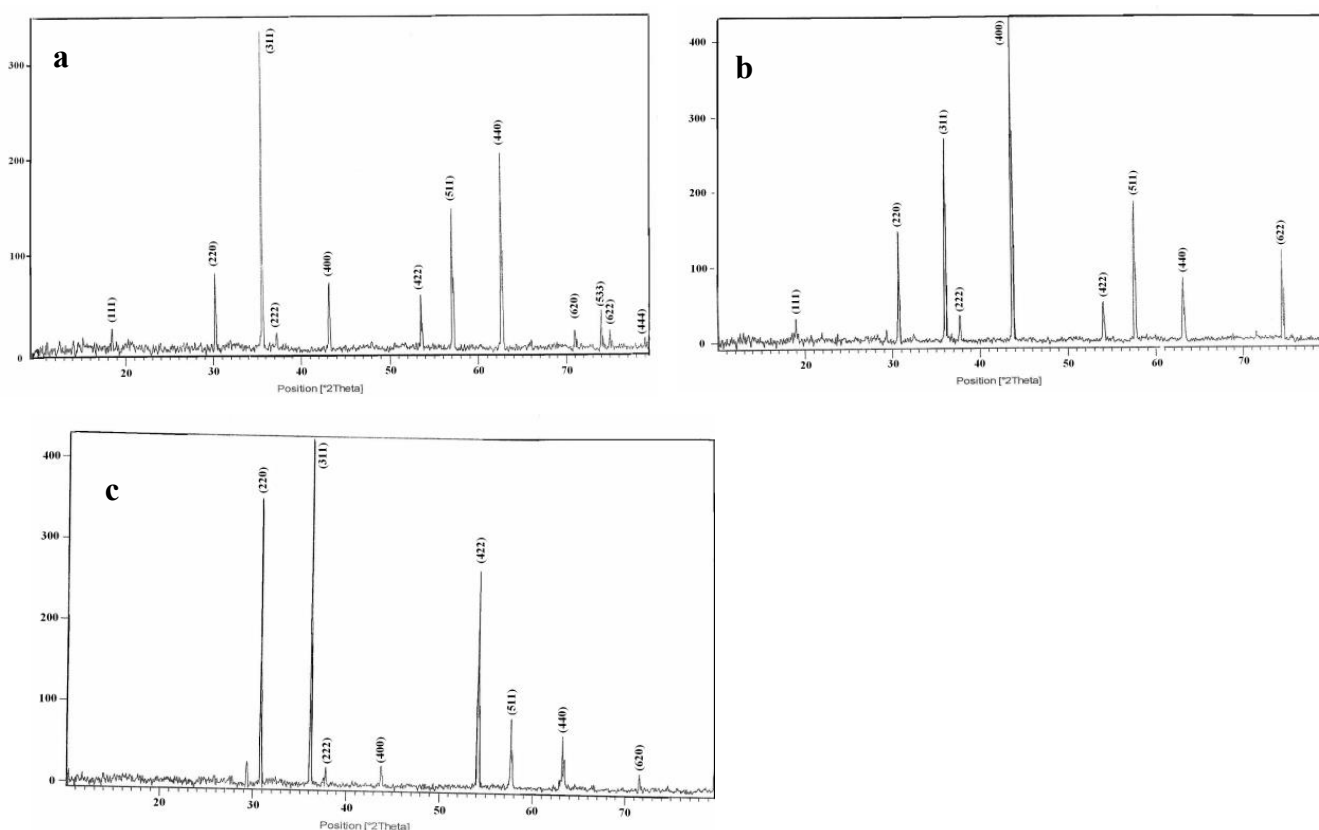


Figure 1: (a) X-ray diffractogram of Sample A; (b) X-ray diffractogram of Sample C; (c) X-ray diffractogram of Sample D.

From earlier investigation of AC-DC electrical conductivities [8] it is observed that the AC conductivity is by band mechanism at all temperatures and AC conductivity decreases with frequency. The dispersion in AC conductivity with frequency has been explained by Koop's theorem [21], which supposed that the ferrites compact acts as a multilayer capacitor. According to Koop's the dielectric constant is inversely proportional to the square root of resistivity. Therefore, increase in dielectric constant with temperature is expected. This behavior is usually interpreted as due to the existence of interfacial polarization [22] which exists in non-homogeneous dielectrics which was explained by Koop's [21] on the basis of Maxwell Wagner [23,24] two layer model.

In this model, considering the dielectric structure consisting of well conducting grains separated by grain boundaries which are poorly conducting. At lower frequencies, grain boundaries are very effective with high resistance giving a very small amount of increment in conductivity. At high frequencies, due to the grain effect there is an increase in conductivity. The total conductivity will be represented by power law [25].

Generally, the impedance data compared (or) fitted to an equivalent circuit, which represents change of physical processes that are taking place in the system an equivalent circuit is made up of passive elements such as capacitors, resistors, inductance and possibly various distributed circuit elements. In such a circuit, capacitance and

inductance will be generally associated with space charge polarization regions. The data obtained in the studies is usually analyzed in terms of four complex formalisms, Viz., The impedance ( $Z'$ ), the electric modulus ( $M'$ ), the admittance ( $Y'$ ) and the permittivity ( $\epsilon'$ ) and these parameters are interrelated by the following relations [26,27].

$$M^* = j\omega C_0 Z^*, \epsilon^* (M^*)^{-1}, Y = (Z^*)^{-1}, Y^* = j\omega C_0 \epsilon^* \quad (1)$$

Where  $\omega$  is the angular frequency,  $C_0$  is the vacuum capacitance of the measuring cell and electrodes with an air gap in place of the sample.

Polycrystalline materials mainly consisting of both large grains and small grain boundary resistances. AC response from the complex impedance plane is dominated by grain boundary resistance i.e., the effect of crystal resistance in  $Z'$  and  $Y'$  were completely mask. In the complex electrical modulus method, i.e.,  $M'$  and  $\epsilon'$ , for the elements that have smallest capacitance will be given more importance. In this case, the response from the crystal dominates the behaviour whereas the grain boundary effects may be masked. Thus, by comparing the results analysis of these two formalisms, it may be possible to separate grain boundaries and bulk effects rather effectively [28]. Especially, ' $Z'$ ' allows for a direct separation of the bulk, grain boundary and electrode phenomena, and also determination of each individual resistance [29].

The room temperature compositional dependence impedance spectra for all the samples investigated are graphically represented in Figure 3. At very low temperature (RT), compositional dependence

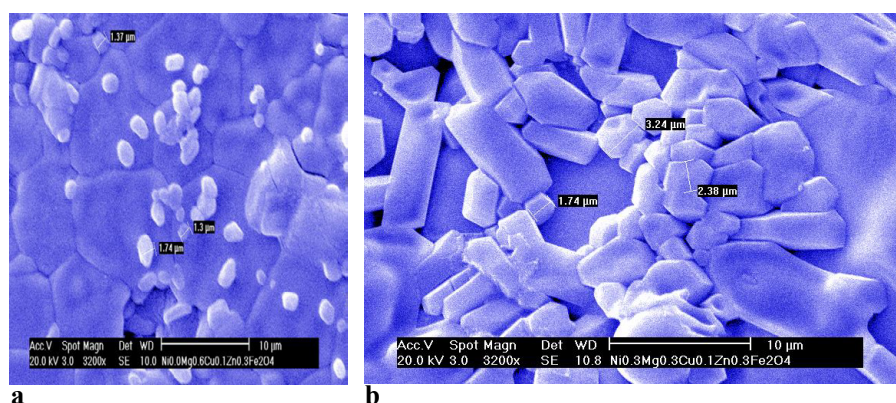


Figure 2: Scanning electron micrographs of (a) Sample A and (b) Sample D.

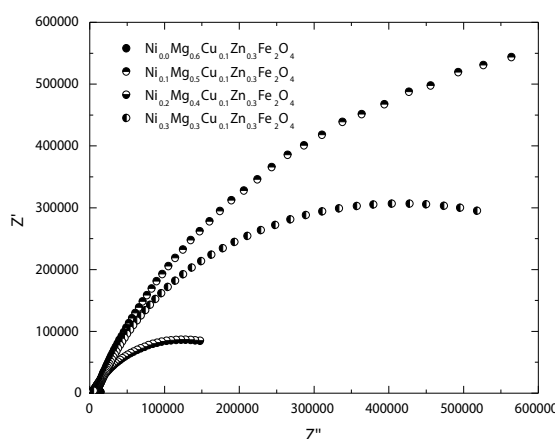


Figure 3: Variation of real and imaginary part of impedance with temperature for  $\text{Ni}_x\text{Mg}_{0.6-x}\text{Cu}_{0.1}\text{Zn}_{0.3}\text{Fe}_2\text{O}_4$  composition at room temperature 30°C.

impedance spectrums for all the samples shows that there is a appearance of a single semi-circular arc whose radius of curvature is dropping down as nickel increases. This indicates that there is arising out of bulk properties in the material. The intercept of semi-circular arcs with the real axis gives sample resistance of the grain and grain boundaries.

Complex impedance spectra analysis (Nyquist plots) which represents the  $Z'$  and  $Z''$  graphical information for all the samples at different temperatures are shown in Figures 4-7, which shows the effect of temperature on impedance behavior, i.e., formation of double semi-circular arcs (Figures 5-7) observed at higher temperatures as the doping of nickel goes on increasing. These two semi circled arc indicates grain and grain boundaries. due to the consequence of the bulk and grain boundary conduction. One can observe the appearance of two single semi-circular arcs whose radius of curvature decreases as temperature increases for the impedance spectrum for  $X = 0.0$  sample. This reveals the existence of the bulk and grain boundary conduction at low temperatures. These semi-circular arcs appear in distinct frequency ranges, one at a higher frequency followed by another lower frequency semi-circular arc. The grain boundary resistance i.e., first semi-circle appears at low frequency region where as the other at high frequencies which corresponds to bulk properties or grain resistance.

This phenomenon is almost similar at different temperatures, also with a difference in the radii of curvature of the arcs, which reduces with a rise in temperature. In the present investigation studies were carried out from 30°C to 350°C with in frequency range of 100 Hz to 1000 K. For pure MgCuZn ferrite at higher temperatures only one semi-circle arc is observed along with a tail which confirms the reduction of bulk and formation of only grain boundaries. Whereas, for the nickel doped samples, first only semi-circular arcs have been observed at low temperature region and two semi-circular arcs have been observed in the high temperature region in impedance spectrum as temperature goes on increasing. The impedance diagram in high frequency regions typically corresponds to the bulk properties of the material and arise due to bulk phenomena, while the low frequency second semicircle has been assigned to the grain boundary conduction [30]. The bulk resistance ( $R_b$ ) increases with rise in temperature. Thus, the bulk conductivity ( $C_b$ ) of the materials decreases with temperature. This kind of behavior in materials is known as positive temperature coefficient of resistance (PTCR) property which is a normal behavior of a semiconductor. The result of impedance spectroscopy measurements of a wide range of frequencies can be presented by several semicircles in the complex  $Z_{\text{Real}}$  and  $Z_{\text{imaginary}}$  plane [31].

Large values of  $Z'$  and  $Z''$  at low frequencies or temperatures

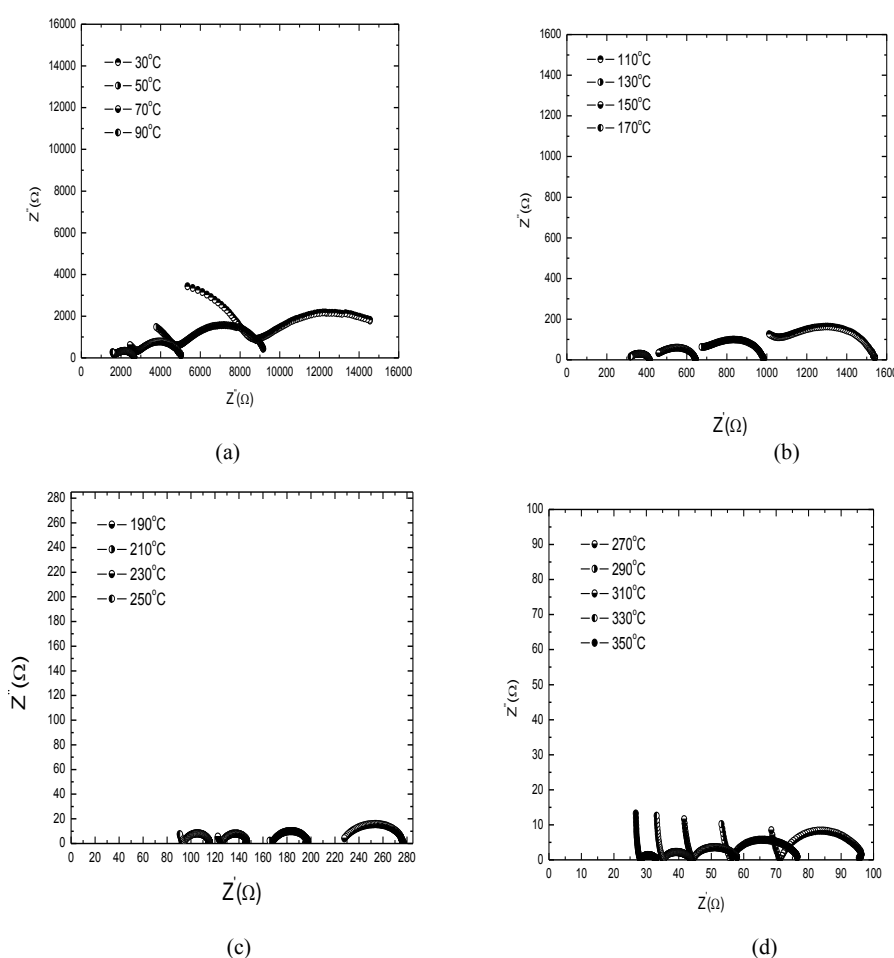
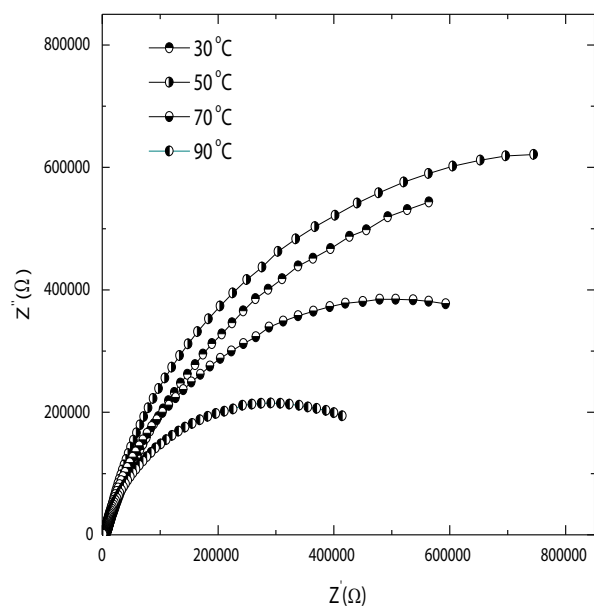
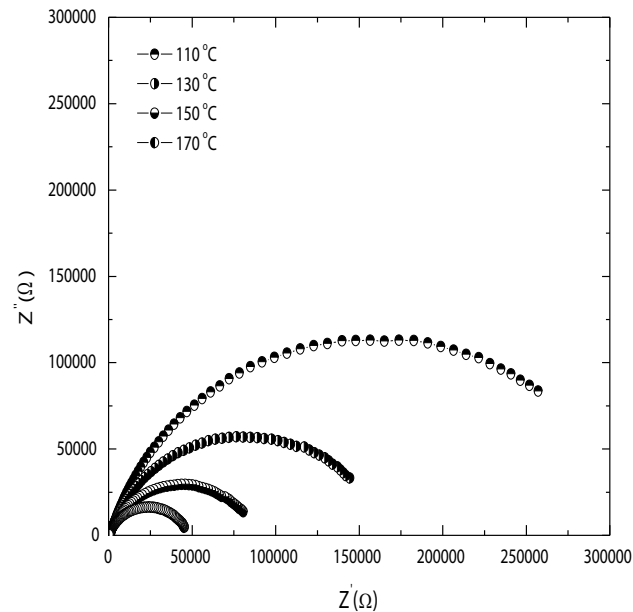


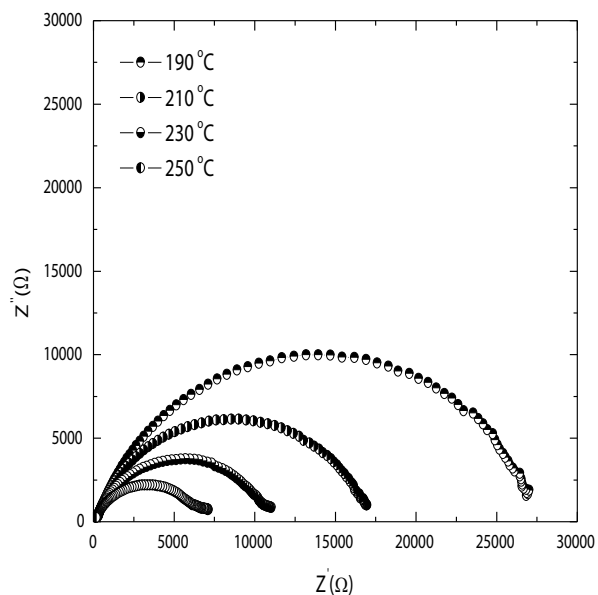
**Figure 4:** (a-d) Variation of real and imaginary part of impedance with temperature for Ni<sub>0.0</sub>Mg<sub>0.6</sub>Cu<sub>0.1</sub>Zn<sub>0.3</sub>Fe<sub>2</sub>O<sub>4</sub> composition within the temperature range 30-350°C.



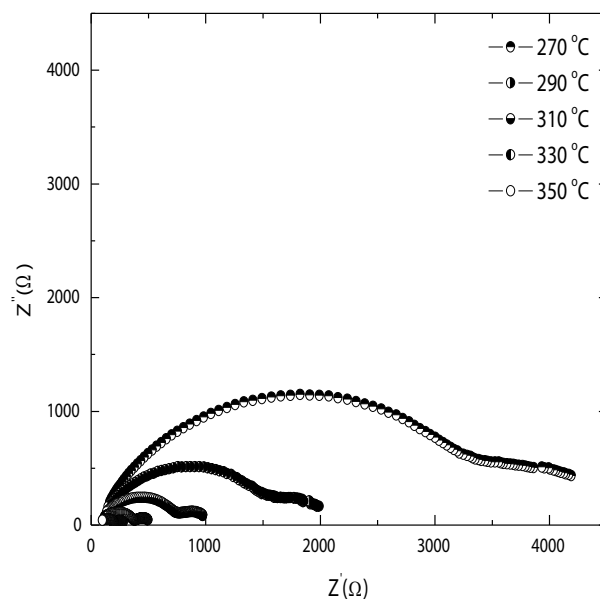
(a)



(b)

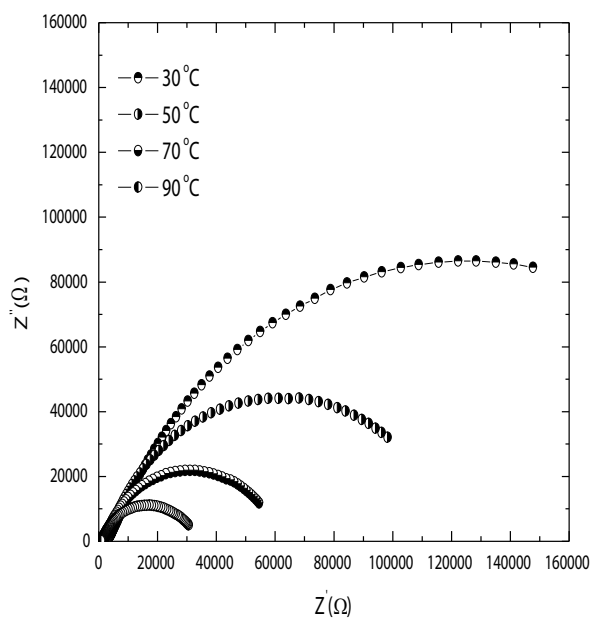


(c)

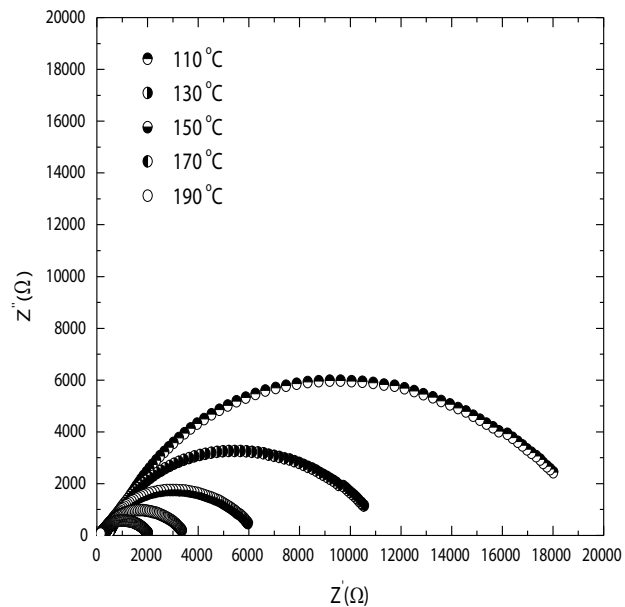


(d)

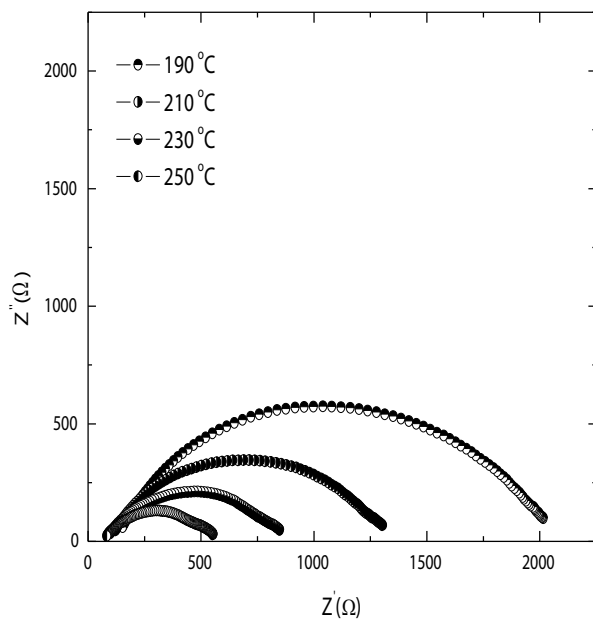
**Figure 5:** (a-d) Variation of real and imaginary part of impedance with temperature for Ni<sub>0.1</sub>Mg<sub>0.5</sub>Cu<sub>0.1</sub>Zn<sub>0.3</sub>Fe<sub>2</sub>O<sub>4</sub> composition within the temperature range 30–350 °C.



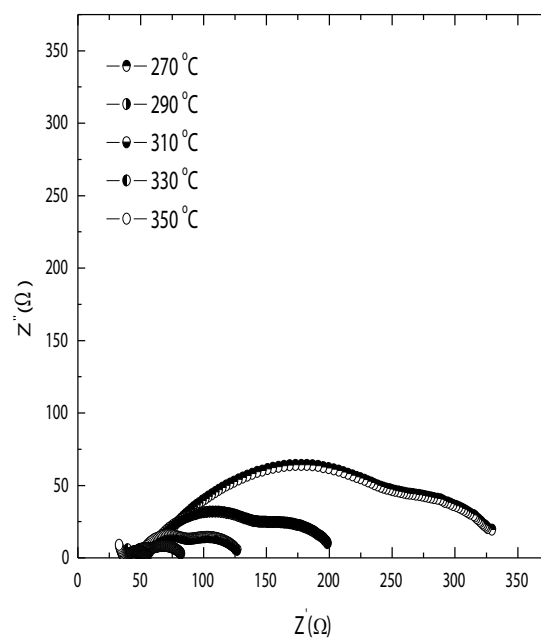
(a)



(b)

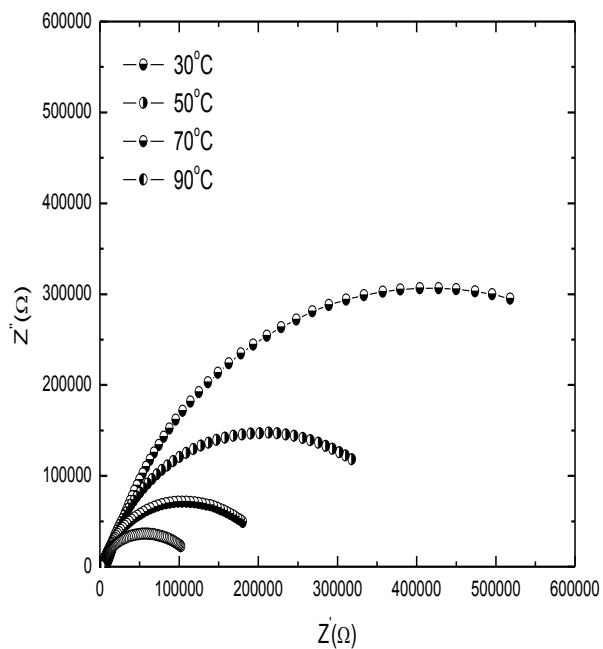


(c)

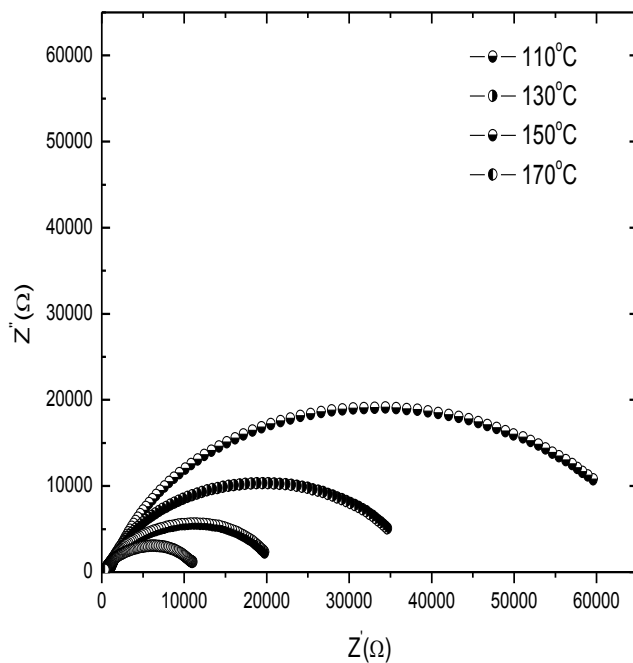


(d)

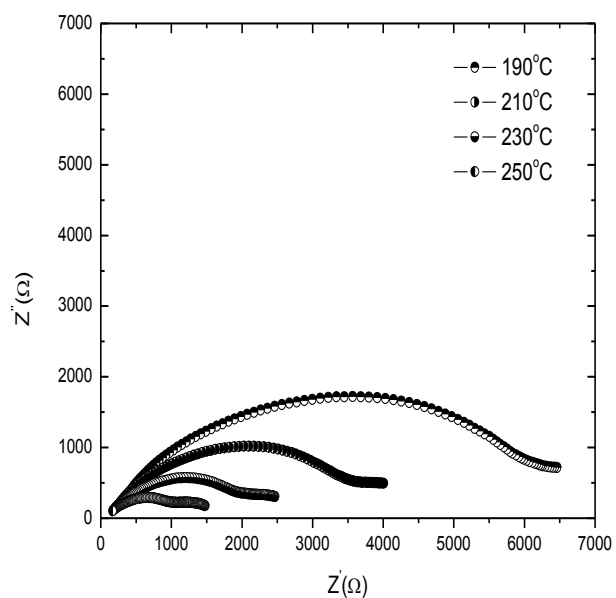
**Figure 6:** (a-d) Variation of real and imaginary part of impedance with temperature for Ni<sub>0.2</sub>Mg<sub>0.4</sub>Cu<sub>0.1</sub>Zn<sub>0.3</sub>Fe<sub>2</sub>O<sub>4</sub> composition within the temperature range 30-350°C.



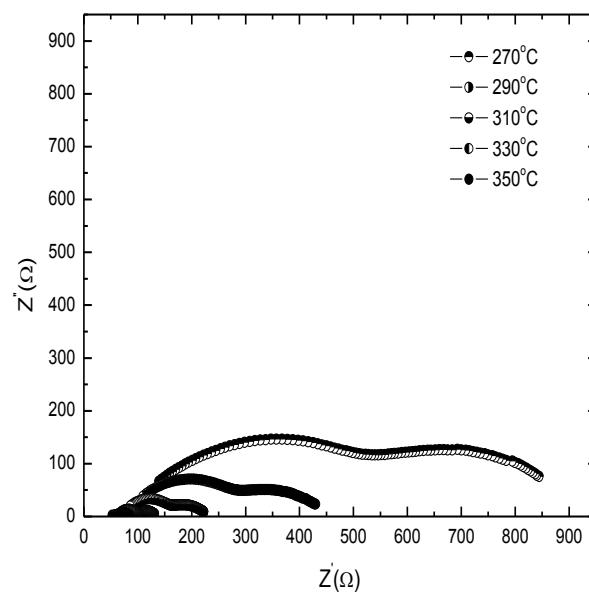
(a)



(b)



(c)



(d)

**Figure 7:** (a-d) Variation of real and imaginary part of impedance with temperature for Ni<sub>0.3</sub>Mg<sub>0.3</sub>Cu<sub>0.1</sub>Zn<sub>0.3</sub>Fe<sub>2</sub>O<sub>4</sub> composition within the temperature range 30-350°C.

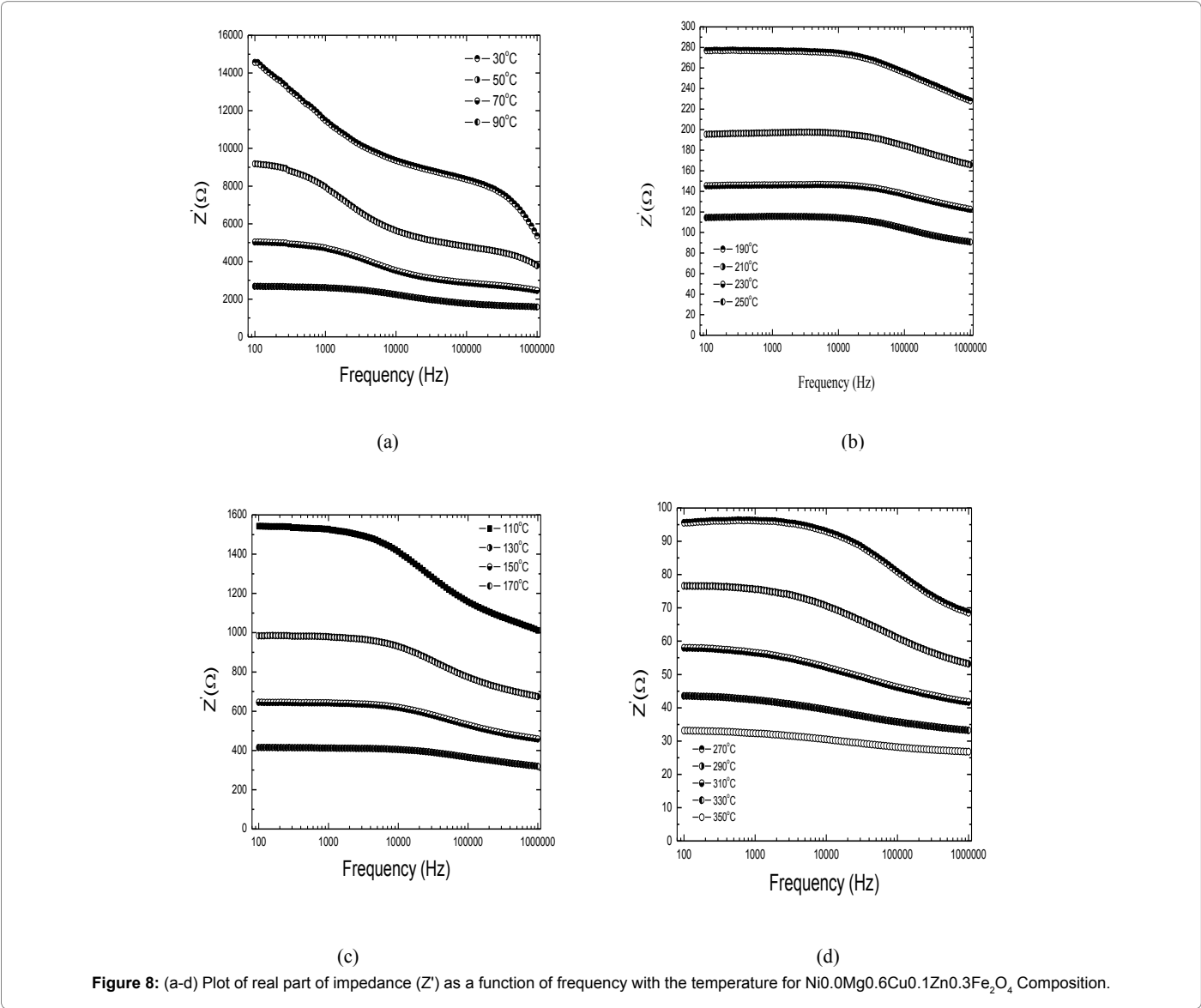
indicates a predominant effect of the polarizations. The intercepts of the two semicircles are used to calculate the bulk resistance ( $R_b$ ) and grain boundary resistance ( $R_{gb}$ ) while the corresponding frequency value evaluated from the apex of the semicircles has been used to calculate the bulk and grain boundary capacitance ( $C_b$ ) using the relation,  $2(f_o R_b C_b) = 1$  and  $2(f_o R_{gb} C_{gb}) = 1$ . Combination of R and C can be either in series or parallel, for a parallel combination of R and C, as temperature increases, both the grain resistance ( $R_b$ ) and grain boundary resistance ( $R_{gb}$ ) is found to decrease with the rise in temperature indicated by a shift in the radius of the semi-circular arcs towards the left side of the real (Z') axis with increase in temperature. The Z' and Z'' plots at higher temperature can be resolved into two semicircles representing two

RC circles in the series given by Cole and Cole [32]. Each semicircle represents the contribution of a particular process such as electrodes and contacts, grain boundaries, grain interior to the total impedance of the sample. Measured values in the form of Nyquist plots are semi-circular. Many of them describe as depressed semicircles with their centering below the x-axis. This phenomenon is called non-Debye relaxation [33]. The values of parameters such as  $R_b$ ,  $R_{gb}$ ,  $C_b$  and  $C_{gb}$  etc., have been reported in the Table 1.

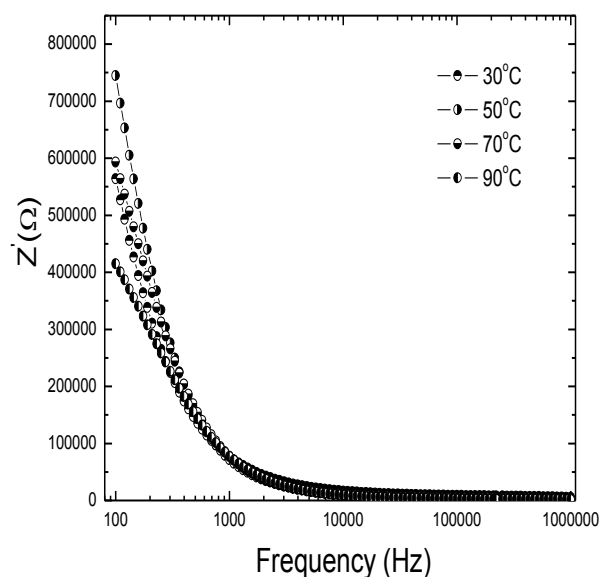
The variables in the real part of impedance (Z') as a function of frequency for all the samples are graphically represented in Figures 8-11. The variation behavior shows a rapid decrease in the value of (Z')

S.No	Sample	F <sub>b</sub>	F <sub>gb</sub>	R <sub>b</sub>	R <sub>gb</sub>	Rho <sub>b</sub>	Rho <sub>gb</sub>	C <sub>b</sub>	C <sub>gb</sub>	EPS <sub>b</sub>	EPS <sub>gb</sub>
1)	A	1000000	631	7100	8300	2.625E3	3.068E3	3.980E-8	3.040E-8	9.362E1	1.273E5
2)	B	100	---	1.35E6	---	4.815E5	---	6.520E-9	---	6.359E3	---
3)	C	158	---	2350000	---	9.420E5	---	4.289E-9	---	1.585E4	---
4)	D	144	---	2790000	---	2.414E6	---	1.400E-9	---	5.174E4	---

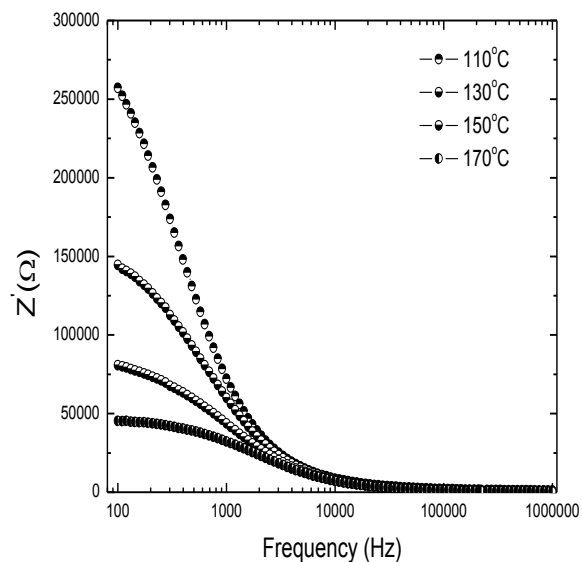
Table 1: Various electrical parameters values for different composition of Ni substituted MgCuZn ferrites at room temperature at 300°C.



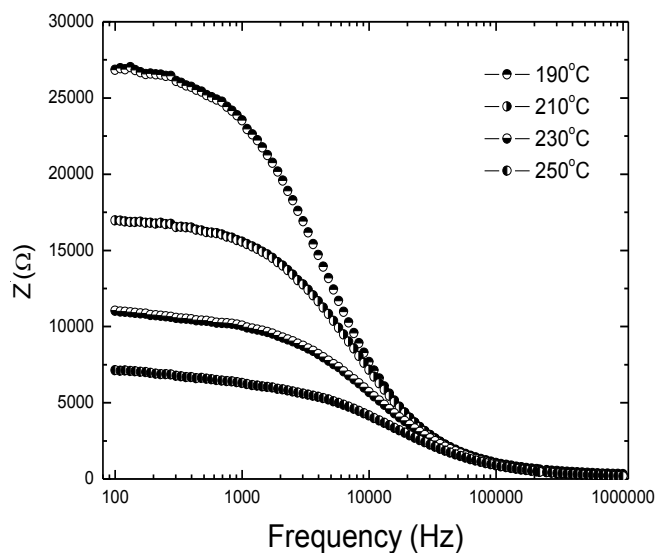




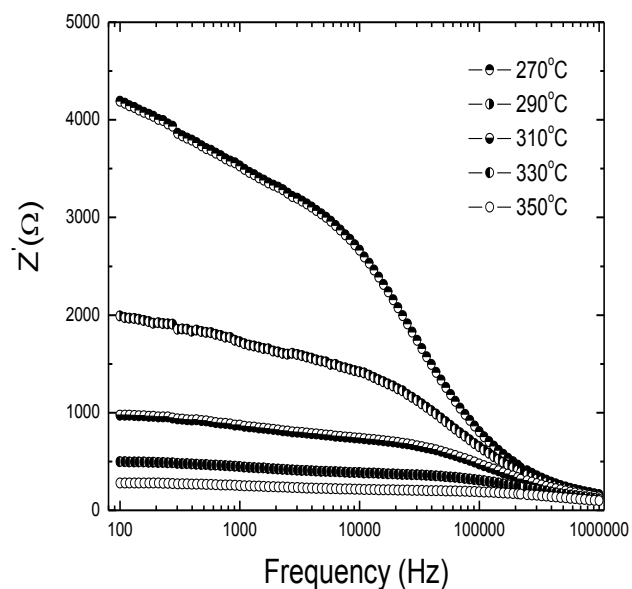
(a)



(b)

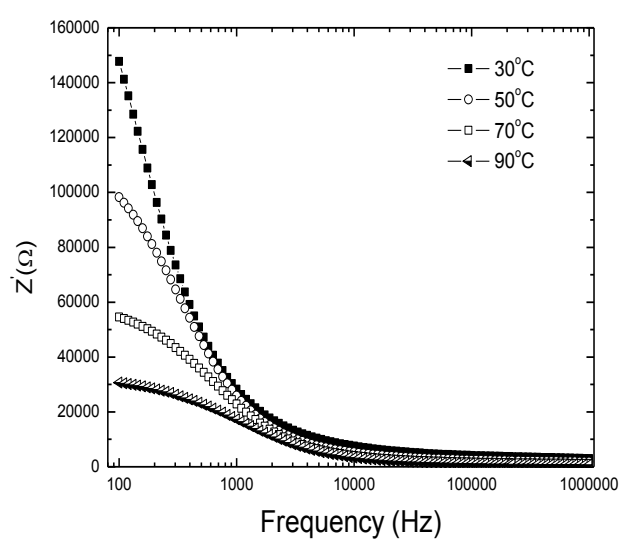


(c)

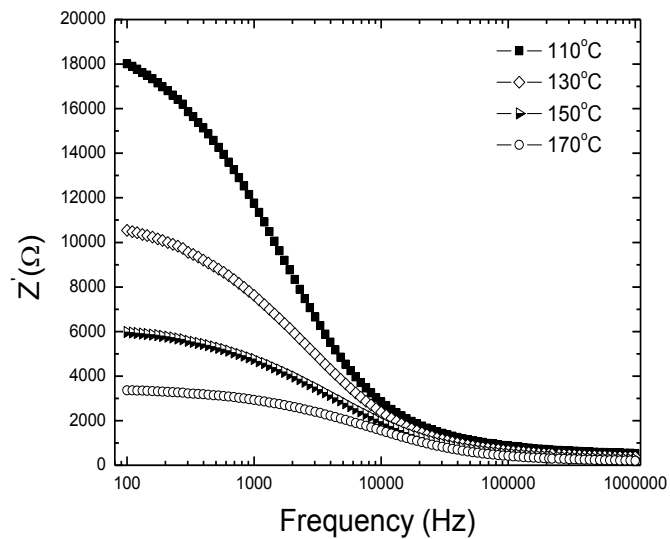


(d)

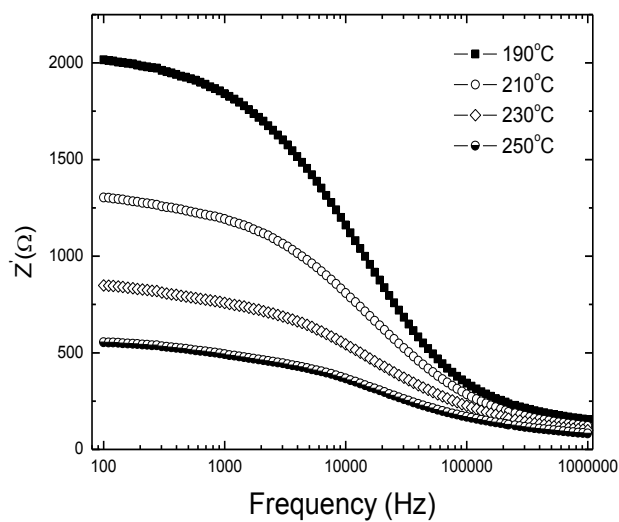
**Figure 9:** (a-d) Plot of real part of impedance ( $Z'$ ) as a function of frequency with the temperature for  $\text{Ni}_{0.1}\text{Mg}_{0.5}\text{Cu}_{0.1}\text{Zn}_{0.3}\text{Fe}_2\text{O}_4$  Composition.



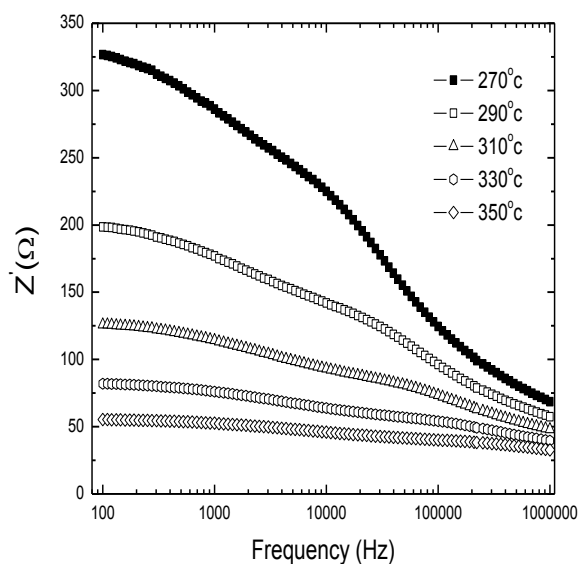
(a)



(b)



(c)



(d)

**Figure 10:** (a-d) Plot of real part of impedance ( $Z'$ ) as a function of frequency with the temperature for  $\text{Ni}_{0.2}\text{Mg}_{0.4}\text{Cu}_{0.1}\text{Zn}_{0.3}\text{Fe}_2\text{O}_4$  Composition.

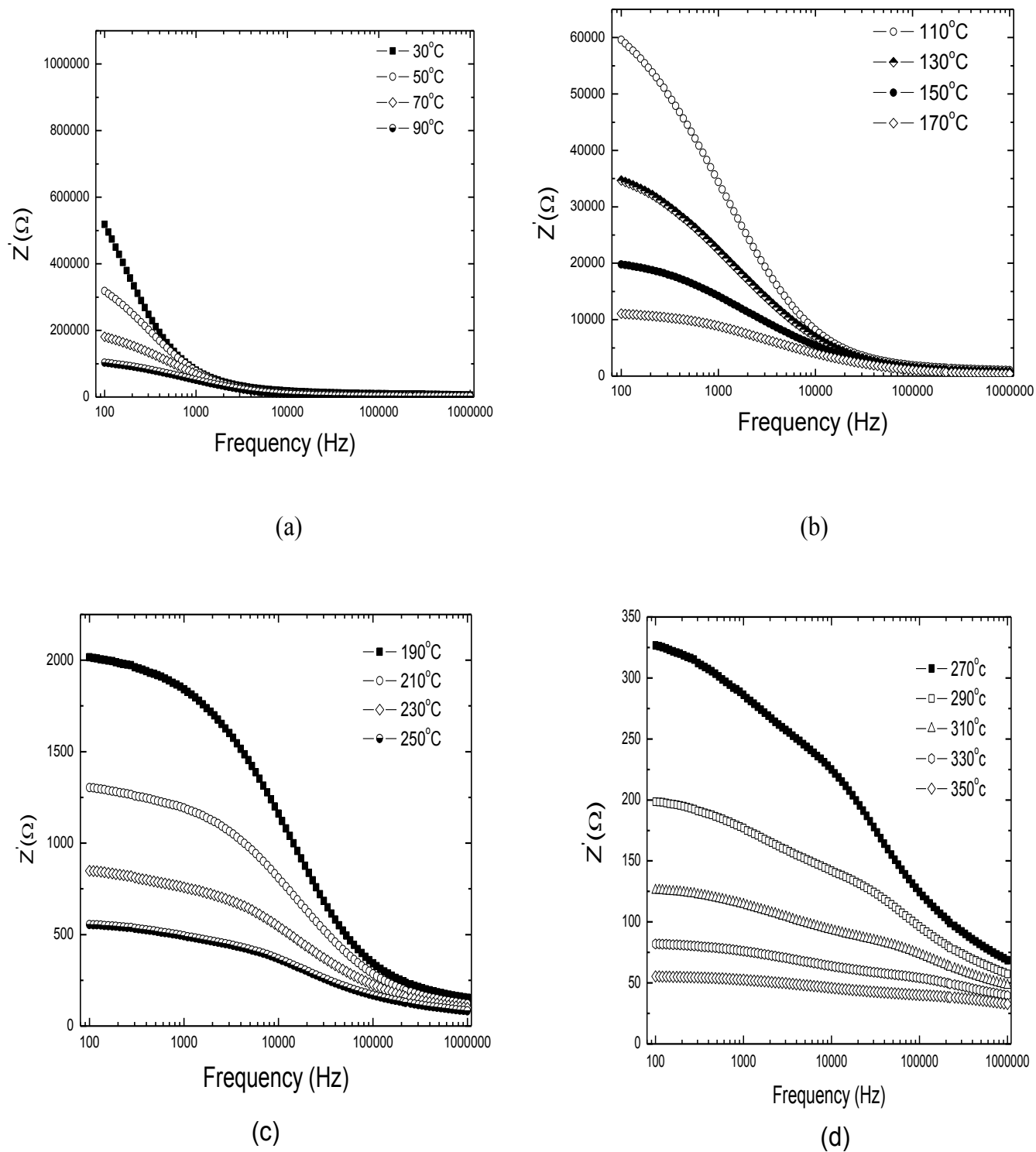


**Figure 11:** (a-d) Plot of real part of impedance ( $Z'$ ) as a function of frequency with the temperature for Ni<sub>0.3</sub>Mg<sub>0.3</sub>Cu<sub>0.1</sub>Zn<sub>0.3</sub>Fe<sub>2</sub>O<sub>4</sub> Composition.

with a rise in the frequency. The impedance value ( $Z$ ) has higher values at lower temperatures in the low frequency region, decreases gradually with a rise in temperature and attains a constant value beyond this frequency i.e. 1MHz. Higher values of ( $Z$ ) at lower frequency and temperature indicated larger effects of space charge polarization and structural defects [34]. The decrease in ( $Z$ ) with the rise in temperature and frequency also indicates a possibility of an increase in the Ac conductivity with an increase in temperature and frequency. The merger between real part of impedance ( $Z'$ ) in the high frequency domain for all temperatures indicate a possibility of the release of space charge as a result of lowering in the barrier properties of the material [35]. These results indicate that electrical conduction will increase from a rise in temperature and the phenomenon is dependent on release of space charge.

Figures 12-15 shows the variation of the imaginary part ( $Z''$ ) of the impedance with frequency (i.e., Loss spectrum) at different temperatures. In these curves, a peak has been observed at lower temperatures in the low frequency region, which further broadened with a rise in temperature and shifting towards higher frequencies. Also the intensity of the peak frequencies decreases with an increase in temperature. A significant asymmetry has also been observed in the peaks and a shift in the peak positions of higher frequency sides of a rise in temperature. The low frequency side of the peak represents the range of frequency in which charge carriers are mobile over long distances. The trend of variation in ( $Z''$ ) with frequency is typical of the presence of electrical relaxation phenomena in the materials which is temperature-dependent. The asymmetric broadening of the peaks suggest the presence of electrical processes of the materials with a

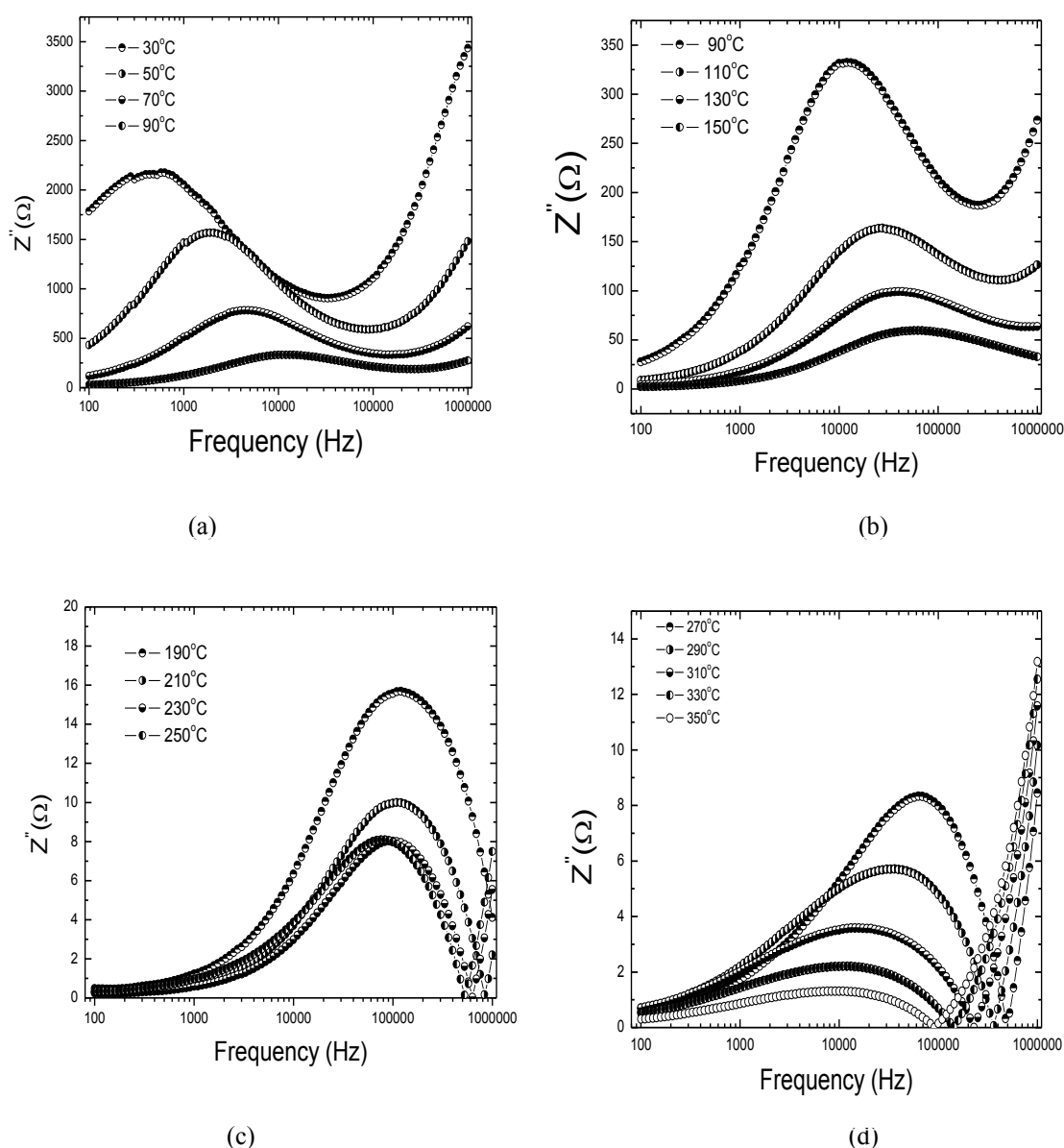
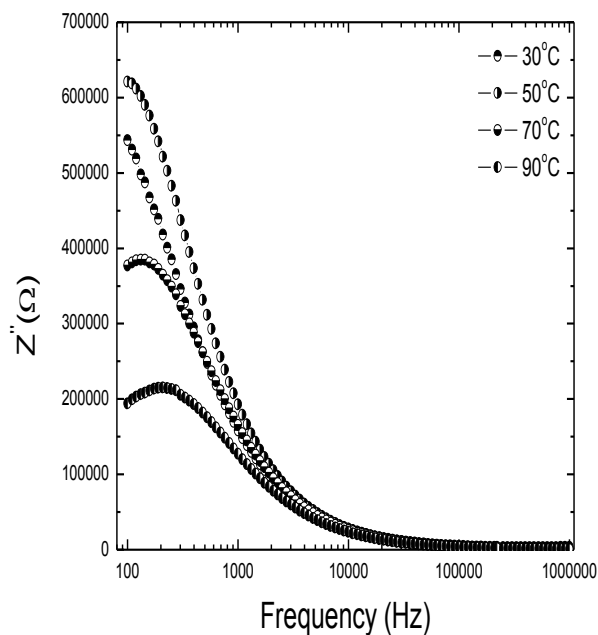
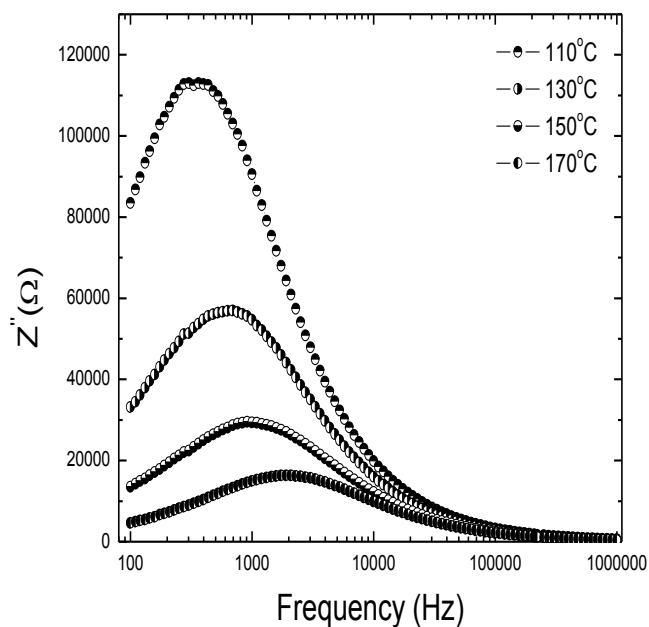


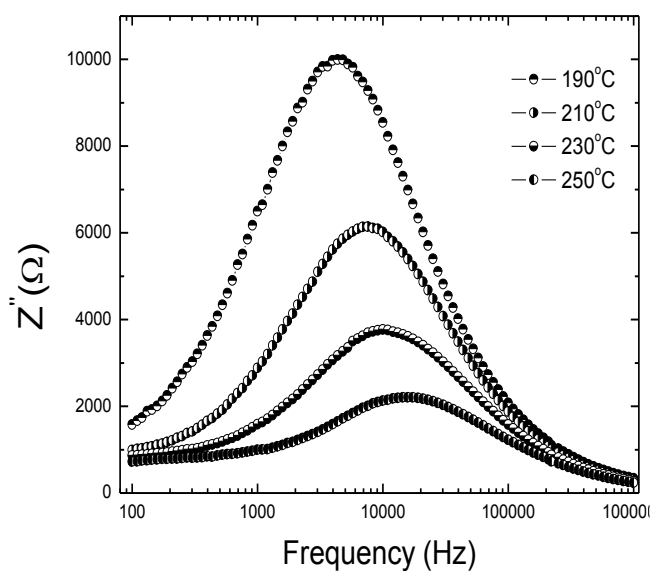
**Figure 12:** (a-d) Variation of imaginary part of impedance the ( $Z''$ ) as a function of frequency with the temperature for  $\text{Ni}_{0.0}\text{Mg}_{0.6}\text{Cu}_{0.1}\text{Zn}_{0.3}\text{Fe}_2\text{O}_4$  Composition.



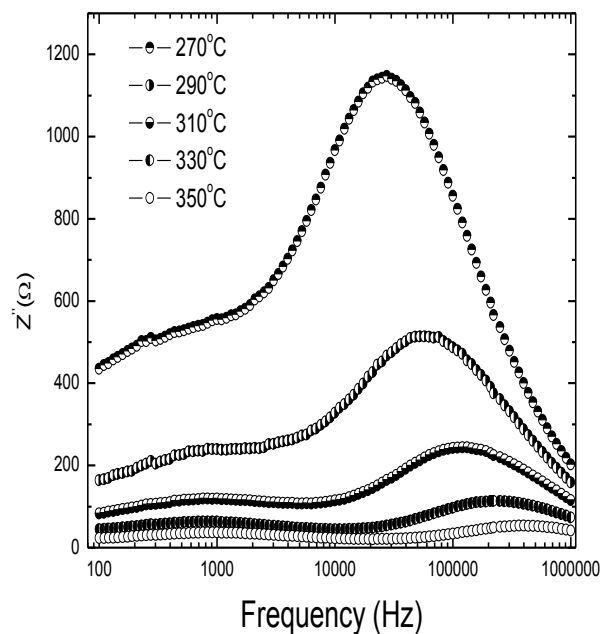
(a)



(b)

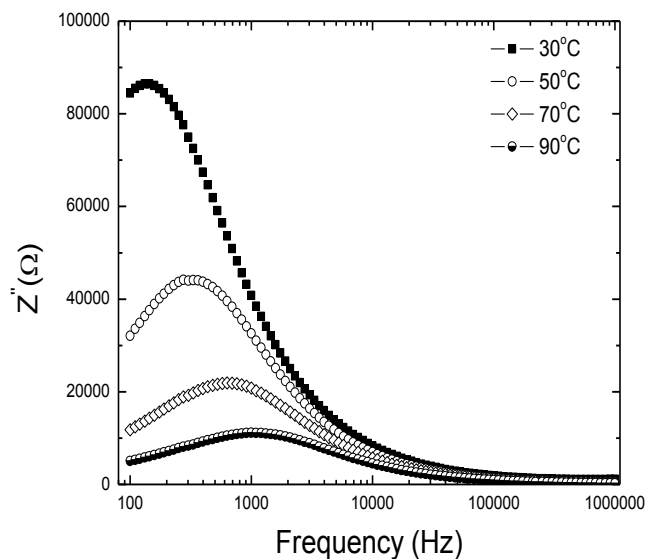


(c)

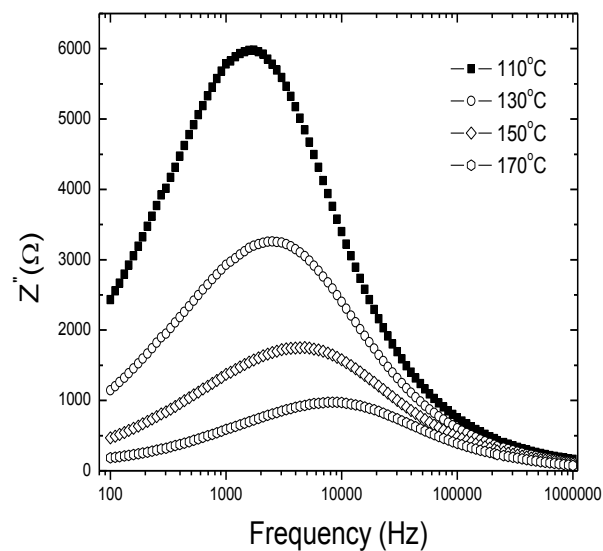


(d)

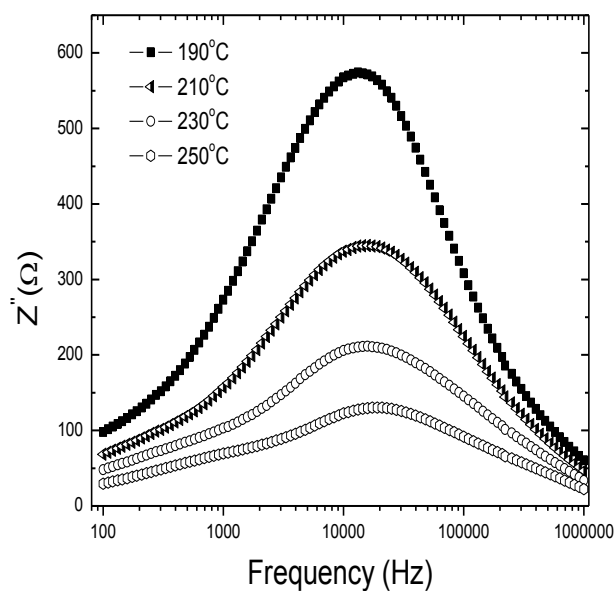
**Figure 13:** (a-d) Variation of imaginary part of impedance the ( $Z''$ ) as a function of frequency with the temperature for  $\text{Ni}_{0.1}\text{Mg}_{0.5}\text{Cu}_{0.1}\text{Zn}_{0.3}\text{Fe}_2\text{O}_4$  Composition.



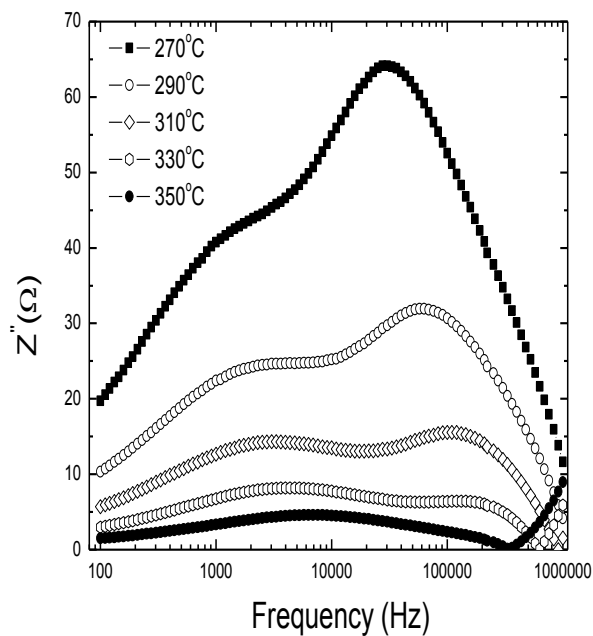
(a)



(b)



(c)



(d)

**Figure 14:** (a-d) Variation of imaginary part of impedance the ( $Z''$ ) as a function of frequency with the temperature for  $\text{Ni}_{0.2}\text{Mg}_{0.4}\text{Cu}_{0.1}\text{Zn}_{0.3}\text{Fe}_2\text{O}_4$  Composition.

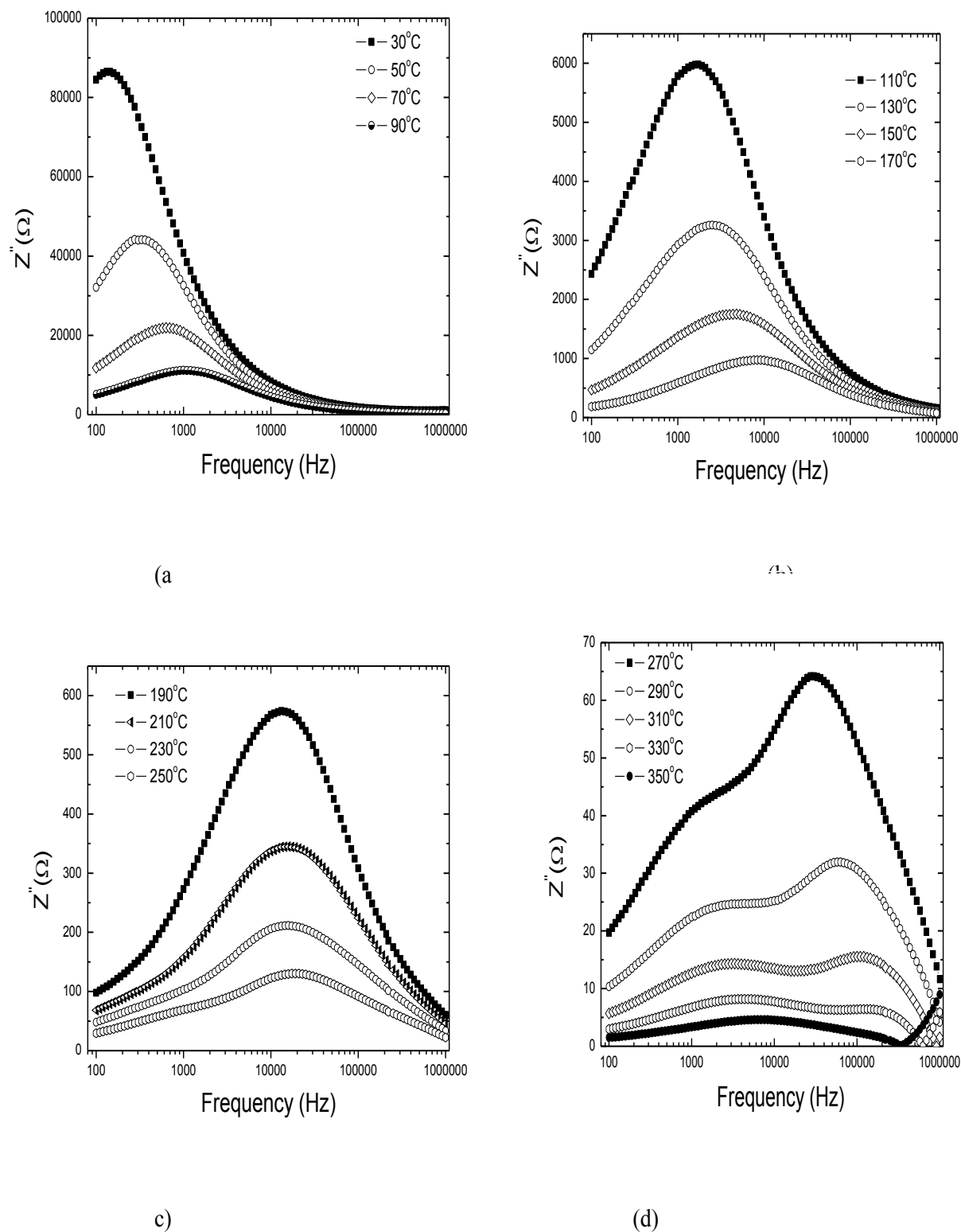


**Figure 15:** (a-d) Variation of imaginary part of impedance the ( $Z''$ ) as a function of frequency with the temperature for  $\text{Ni}_{0.3}\text{Mg}_{0.3}\text{Cu}_{0.1}\text{Zn}_{0.3}\text{Fe}_2\text{O}_4$  Composition.

spread of relaxation time [36]. The shifting of peaks indicates that the net relaxation time is decreasing from the increase in temperature.

## Conclusions

The Nickel doped MgCuZn ferrites compounds were prepared from a high-energy ball-milling method followed by conventional method. Preliminary structural studies suggest that the crystal system of parent compounds remains same (cubic spinel system). Complex impedance spectroscopy, in terms of a simultaneous analysis of the complex impedance was used to investigate the electrical behavior of NiMgCuZn ceramics. Complex impedance spectra indicated about the possible contribution to the bulk and grain boundaries from room temperature to higher temperatures and also about the temperature-dependent relaxation phenomena.

Bulk resistance ( $R_b$ ) increases (and  $Rho_b$ ) with increase in Ni content. Bulk capacitor ( $C_b$ ) and bulk frequency ( $F_b$ ) decreases with increase in Ni concentration.  $EPS_b$  also decreases with increase in Ni composition. Where as grain boundary parameters  $F_{gb}$ ,  $R_{gb}$ ,  $Rho_{gb}$ ,  $C_{gb}$  and  $EPS_{gb}$  can be seen for Pure MgCuZn ferrite and it disappears with the increase of Ni Concentration.

With an increase of Ni composition the materials behaves like positive temperature coefficient of resistance as resistance in the both cases increases.

## References

- Zaki HM (2005) AC conductivity and frequency dependence of the dielectric properties for copper doped magnetite. *Phys B* 363: 232-244.
- Shaikh AM, Kanamadi CM, Chougule BK (2005) Electrical resistivity and thermoelectric power studies on Zn-substituted Li-Mg ferrites. *Mater Chem Phys* 93: 548-551.
- Dias A, Moreira RL (1998) Conductivity behavior of n-type semiconducting ferrites from hydrothermal powders. *J Mater Res* 13: 2190-2194.
- Kadam SL, Kanamadi CM, Patankar KK, Chougule BK (2005) Dielectric behaviour and magnetoelectric effect in  $Ni_{0.5}Co_{0.5}Fe_2O_4 + Ba_{0.8}Pb_{0.2}TiO_3$  ME composites. *Mater Lett* 59: 215-219.
- Nanba N, Kobayashi S (1978) Semiconductive Properties and Cation Distribution of Copper Ferrites  $Cu_{1-5}Fe_2 + 5O_4$ . *Jpn J Appl Phys* 17: 1819.
- Hoque SM, Choudhury MA, Islam MF (2002) Effect of cobalt substitution on the properties of nickel-copper ferrite. *J Magn Magn Mater* 251: 293-303.
- Rezlescu N, Rezlescu E (1974) Dielectric properties of copper containing ferrites. *Phys Status Solidi (a)* 23: 575-582.
- Varalaxmi N, Sivakumar KV (2010) Studies on AC and DC electrical conductivity and thermo-electric power of NiMgCuZn ferrites. *Int J Nanopart* 3: 349-366.
- Ghodake UR, Rahul C Kambaleb, Suryavanshic SS (2017) Effect of  $Mn^{2+}$  substitution on structural, electrical transport and dielectric properties of Mg-Zn ferrites. *Ceram Int* 43:1129-1134.
- Penchal Reddy M, Venkata Ramana M, Rama Manohar Reddy N, Siva Kumar KV, Rama Krishna Reddy R (2011) Structural, Electrical and Magnetic Characterization of Ni-Cu-Zn Spinel Ferrites. *Mod Phys Lett B* 25: 211-222.
- Kabbur SM, Ghodake UR, Kambale RC, Sartale SD, Chikhale LP, et al. (2019) Structural, magnetic, optical properties and cation distribution of nanosized  $Ni_{0.3}Cu_{0.3}Zn_{0.4}Tm_xFe_{2-x}O_4$  ( $0.0 \leq x \leq 0.10$ ) spinel ferrites synthesized by ultrasound irradiation. *Electron Mater*.
- Sujatha C, Reddy KV, Babu KS, Reddy ARC, Suresh MB, et al. (2013) Effect of co substitution of Mg and Zn on electromagnetic properties of NiCuZn ferrites. *J Phys Chem Solids* 74: 917-923.
- Hossain AA, Biswas TS, Mahmud ST, Yanagida T, Tanaka H, et al. (2009) Influence of Mg and Cr substitution on structural and magnetic properties of polycrystalline  $NiO_{0.5}Zn_{0.5} - x - yMgxCr_yFe_2O_4$ . *Mater Chem Phys* 113: 172-178.
- Reddy MP, Madhuri W, Reddy NR, Kumar KS, Murthy VRK, et al. (2010) Influence of copper substitution on magnetic and electrical properties of MgCuZn ferrite prepared by microwave sintering method. *Mater Sci Eng: C* 30: 1094-1099.
- Akhter S, Paul DP, Akhter S, Saha DK, Hoque SM, et al. (2014) Structural, Magnetic and Electrical Properties of Cu-Mg Ferrites. *Sci Res* 6: 205-215.
- Nakamura T, Naoe M, Yamada Y (2006) Complex impedance spectra of chip inductor using Li-Zn-Cu-Mn ferrite. *J Magn Magn Mater* 305: 120-126.
- Khoun TF, Hassan J, Abd Z, Wahab Raba'ah Syahidah Aziz (2016) Engineering Science and Technology, an International J.
- Loyau V, Wang GY, Lobue M, Mazaleyrat F (2012) An analysis of Mn-Zn ferrite microstructure by impedance spectroscopy, scanning transmission electron microscopy and energy dispersion spectrometry characterizations. HAL Id: hal-hal-00738002.
- Mazen SA, Abu-Elsaad NI (2017) Dielectric properties and impedance analysis of polycrystalline Li-Si ferrite prepared by high energy ball milling technique. *J Magn Magn Mater* 442: 72-79.
- Varalaxmi N, Sivakumar KV (2011) The Role of Ni and Mg on the Dielectric properties of CuZn Ferrites Developed for Microinductor Applications. *Int J Electr Electron Comp Tech* 1: 20-28.
- Koops CG (1951) On the Dispersion of Resistivity and Dielectric Constant of Some Semiconductors at Audiofrequencies. *Phy Rev* 83: 121.
- Abdullah MA, Yusoff AN (1996) Complex impedance and dielectric properties of an MgCuZn ferrite. *J Alloys Comp* 233: 129-135.
- Maxwell JC (1973) Electricity and Magnetism. J Oxford University Press, Oxford, London.
- Wagner KW (1913) Zur theorie der unvollkommenen dielektrika. *Ann Phys* 345: 817-855.
- Mott NF, Davis EA (1979) Electronic Processes in Non-Crystalline Materials. Clarendon Press, Oxford, Great Britain.
- Abram EJ, Sinclair DC, West AR (2003) A strategy for analysis and modelling of impedance spectroscopy data of electroceramics: doped lanthanum gallate. *J Electroceram* 10: 165-177.
- Sinclair DC, West AR (1989) Impedance and modulus spectroscopy of semiconducting  $BaTiO_3$  showing positive temperature coefficient of resistance. *J Appl Phys* 66: 3850-3856.
- James AR, Kumar GS, Suryanarayana SV, Bhimasankaram T (1996) Impedance spectroscopic studies in  $SrBi_5FeTi_4O_{18}$ . *Ferroelectrics* 189: 81-90.
- James AR, Priya S, Uchino K, Srinivas K (2001) Dielectric spectroscopy of Pb (Mg 1/3 Nb 2/3) O 3-PbTiO 3 single crystals. *J Appl Phys* 90: 3504-3508.
- Irvine JTC, Sinclair DC, West AR (1990) Electroceramics: Characterization by Impedance Spectroscopy. *Adv Mater* 2: 132-138.
- Jiang SP, Love JG, Badwal SPS (1997) Electrochemical Techniques in Studies of Solid Ionic Conductors. *Key Eng Mater* 125: 81-132.
- Cole KS, Cole RH (1941) Dispersion and absorption in dielectrics I. Alternating current characteristics. *J Chem Phys* 9: 341-351.
- Alim MA (1989) Admittance-Frequency Response in Zinc Oxide Varistor Ceramics. *J Am Ceram Soc* 72: 28-32.
- Chaudhry MA, Jonscher AK (1988) High-temperature dielectric properties of ruby mica perpendicular to the cleavage planes. *J Mater Sci* 23: 208-216.
- Maier J (2003) Defect chemistry and ion transport in nanostructured materials: Part II. Aspects of nanoionics. *Solid State Ionics* 157: 327-334.
- Idem J (1981) *Mater Sci* 16: 775.